Received: 1 February 2024 | Revised: 29 March 2024 | Accepted: 4 April 2024

DOI: 10.1002/eng2.12903

RESEARCH ARTICLE

Engineering Reports Open Access WILEY

Broadband multi-layered stepped cone shaped metamaterial absorber for energy harvesting and stealth applications

Mehmet Bağmancı[1] | Lulu Wang[2] | Cumali Sabah[3] | Muharrem Karaaslan[1] | Liton Chandra Paul[4] | Tithi Rani[5] | Emin Unal[1]

[1]Electrical and Electronics Engineering, Iskenderun Technical University, Iskenderun, Hatay, Turkey

[2]Biomedical Device Innovation Center, Shenzhen Technology University, Shenzhen, China

[3]Electrical and Electronics Engineering, Middle East Technical University-Northern Cyprus Campus, Mersin, Turkey

[4]Electrical, Electronic and Communication Engineering, Pabna University of Science and Technology, Pabna, Bangladesh

[5]Electronics and Telecommunication Engineering, Rajshahi University of Engineering and Technology, Rajshahi, Bangladesh

Correspondence
Liton Chandra Paul, Electrical, Electronic and Communication Engineering, Pabna University of Science and Technology, Pabna, Bangladesh.
Email: litonpaulete@gmail.com

Abstract

In this study, a broadband polarization and angle-independent metamaterial absorber (MA) is investigated in the microwave range. It is made up of a periodic array of multi-layered metal-dielectric stepped cones. Since the dimensions of the layers forming the unit cell are different, each layer resonates at different frequencies with overlapping bands. The overall response of the structure, with its extremely wide bandwidth, can be obtained by summing all the overlapping frequency responses corresponding to each layer. In numerical simulation, it is observed that the absorption at normal incidence is above 90% in the frequency range between 9.68 and 17.45 GHz and 95% in the frequency range between 9.91 and 14.86 GHz. The energy harvesting ratios of the structure are also evaluated in a wide spectral band. A power ratio of around 90% is obtained in the same frequency range in accordance with absorption response. A noticeable harvesting efficiency of up to 82% is observed, which represents the energy level converted into electrical energy on resistors.

KEYWORDS

broadband metamaterial absorber, cone-shape, energy harvesting, multi-layer, stealth applications

1 | INTRODUCTION

Metamaterials have exotic electromagnetic features. The unusual electromagnetic features of metamaterials, such as their negative dielectric constant and negative permeability, are not present in natural materials.[1] These are electromagnetic materials that have been synthesized and are made up of resonant elements that are subwavelength in size.[2] Metamaterials find applications in various areas, such as sensors,[3,4] camouflage,[5–7] invisibility cloak,[8–10] perfect absorber,[11–13] and energy harvesting.[14–16] Among these, metamaterial absorbers (MAs) have attracted significant attention because of their superiority, perfect absorption, ease of manufacture, and flexible design ability.[17,18] But most of the MAs developed in the microwave regime have a narrow absorption bandwidth. Actually, the design of a broadband MA is very troublesome due to the complex interactions among the various resonant units placed in a limited space.[19,20] In addition, another problem encountered in designing is the conflict between bandwidth and absorption strength.[21] In order to harvest energy from electromagnetism, the author presented a spiral ring-shaped 20×20 unit cell metamaterial structure with an absorption ratio exceeding 90% employing 400 Ω lumped resistance.[22] An electrical dimension of $0.18\lambda_0 \times 0.18\lambda_0 \times 0.019\lambda_0$ for a CSRR-based metamaterial in the S and C satellite bands was investigated by varying the load resistance between each ring resonator's gaps.[23] The authors of Reference 24 discussed the obstacles and future directions for mechanical and acoustic metamaterials in energy harvesting and sensing applications. An electromechanically coupled metamaterial-based piezoelectric energy harvesting system was studied in Reference 25. The substantial birefringence and transmission efficiency of metasurfaces are used to illustrate an efficient design technique[26] for a transmissive Airy optical beam generator. It is possible to simultaneously adjust the local amplitude and phase of transmitted light to satisfy the Airy function, regardless of the incidence wavelength, by varying the orientation angles of silicon nano-pillars. With a sensitivity of roughly 5.9 and 6.4 GHz/K, respectively, a dual-band THz absorber based on metamaterials constructed in a vertical square split ring (VSSR) shape was investigated for a temperature sensor.[12] In Reference 27, a plasmonic light absorber consisting of an all-dielectric GaAs cylinder resonator adhered to an ultra-thin GaAs spacer layer backed with a tungsten substrate was investigated. With a stronger circular dichroism effect based on temperature-tunable InSb,[28] the investigators proposed a THz chiral metasurface absorber made of a periodic array of developed C-shaped InSb attached to a copper sheet for improved applications in sensing.

Therefore, we have proposed a new 3D non-planar MAs by integrating known absorber structures with overlapping frequency responses working in the GHz frequency spectrum. Due to the disadvantages of conventional metamaterials, in the proposed study, we proposed layered MAs, of which the overall response having an extremely wide bandwidth can be achieved by adding every frequency of overlapping responses to layers. The proposed multi-layered MAs simultaneously improve both bandwidth and absorption.

2 | DESIGN OF METAMATERIAL ABSORBER

In this study, we proposed a broadband structure in the microwave frequency band. The suggested structure is composed of multi-layered metallic-dielectric stepped cones. The schematic of the proposed 3D structure, consisting of 20 circular layers with different radiuses, is shown in Figure 1A. Each layer of varying size contains a metal plate placed on a dielectric substrate. The backside of the widest layer at the bottom is assigned a metallic layer to prevent transmission. A unit cell of the multi-layered MA is shown in Figure 1B. The cone shape was chosen for its central symmetry to provide responses independent of azimuth angle. The metallic background in the absorber is copper, which has an electrical conductivity of $\sigma = 5 \times 10^7$ S/m. The dielectric layer is chosen as FR4, whose dielectric constant and loss tangent are = 4.3 and $\tan\delta = 0.025$, respectively. To provide broad band absorption characteristics, the sizes are evaluated using a parametric study and genetic algorithm.

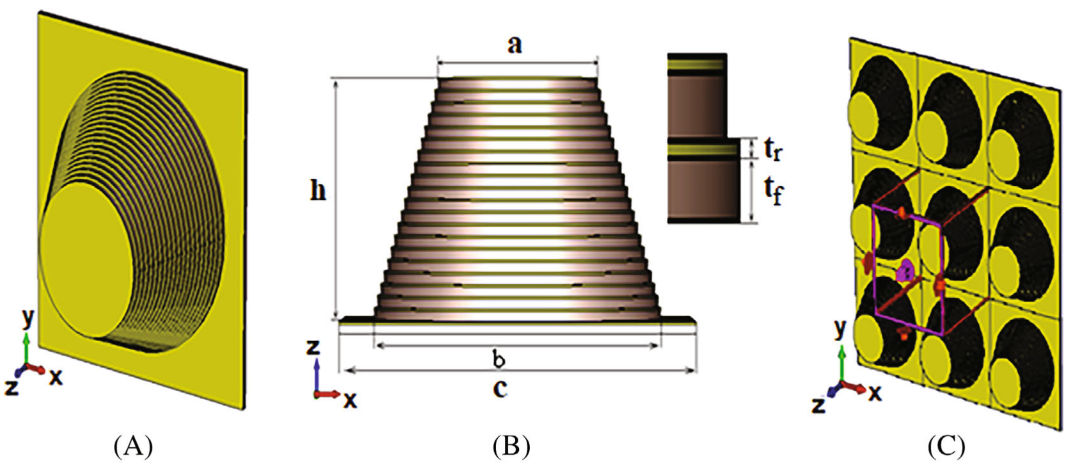

FIGURE 1 (A) 3D observation of the absorber, (B) side view of the absorber and unit cell dimensions (inset on right), and (C) simulation adjustments as boundary conditions. The evaluated dimensions of one unit cell are $a = 5$ mm, $b = 8.99$ mm, $c = 11$ mm, $h = 5$ mm, $t_r = 0.05$ mm, and $t_f = 0.2$ mm.

3 | NUMERICAL ANALYSIS AND DISCUSSION

In this study, the simulations have been carried out using a finite integration technique-based simulator. To obtain reflection and absorption characteristics in the wide band, use the optimum dimensions shown in Figure 1C, which are used in numeric simulation. Periodic boundary conditions are used in the x and y directions to provide periodicity for TE and TM incident cases and open (add space) along the z direction where the incident wave is applied. The electric field component is directed along the y-direction (TE) as the excitation wave. The frequency characteristics of absorption $A(w)$ can be calculated using the following formula:

$$A(\omega) = 1 - R(\omega) - T(\omega), \tag{1}$$

where, $R(\omega)$ and $T(\omega)$ are frequency dependent reflection and transmission values. In order to improve the absorption of structure, both reflection $R(\omega) = |S_{11}^2|$ and transmission $T(\omega) = |S_{21}^2|$ must be reduced at the resonance frequency region. Due to the metal background along the back side of the structure, the transmitted waves have been blocked. Hence, the absorption is solely related to the reflection value; therefore, the reflection properties of the absorber are investigated to observe the effectiveness of the absorber. As a result, the simulation results of the absorber with optimized dimensions have been obtained according to the revised equation of absorption $A(\omega) = 1 - R(\omega)$ where $|S_{21}^2| = 0$, since transmission value is neglected. The reflection and absorption properties of the absorber are depicted in Figure 2.

It can be seen in Figure 2 that each layer consisting of copper film and FR4 as a substrate creates an absorption peak in the absorption spectrum with an absorptivity above 98% in the frequency range of 10–17.5 GHz. It shows an extremely wide absorption and reflection bandwidth. Despite having a very wide bandwidth, to achieve a more meaningful result, one should calculate the relative absorption bandwidth (W_{RAB})[29] using the following equation.

$$W_{\mathrm{RAB}} = 2(f_{Max} - f_{Min})/(f_{Max} + f_{Min}). \tag{2}$$

The frequency range corresponding to maximum absorption includes part of the X band; therefore, the proposed structure has potential application for stealth technology. It is well known that a high absorption value can be achieved under certain conditions, such as a minimum transmission coefficient provided by a backward metallic sheet and a minimum reflection value achieved by impedance matching. Impedance matching can be achieved by matching the overall system impedance with the free space of low loss characteristics.[30]

The electric and magnetic field distributions of the structure are shown in Figure 3A,B, respectively. It is well known that the resonant frequency of an object depends on its structure. Since the dimensions of the layers are different, each layer of the unit cell resonates with the incident wave at sliding frequencies that combine with each other. The response of the absorber is evaluated by adding the overlapping frequency responses belonging to each layer. It is obvious that at a specific frequency, the electric and magnetic fields are localized at the corresponding part of the stepped cone. The

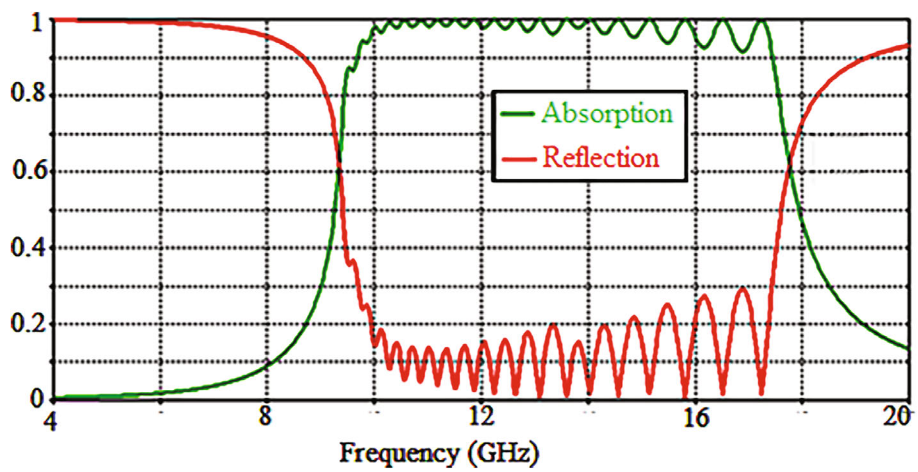

FIGURE 2 Reflectivity and absorptivity values of the suggested absorber.

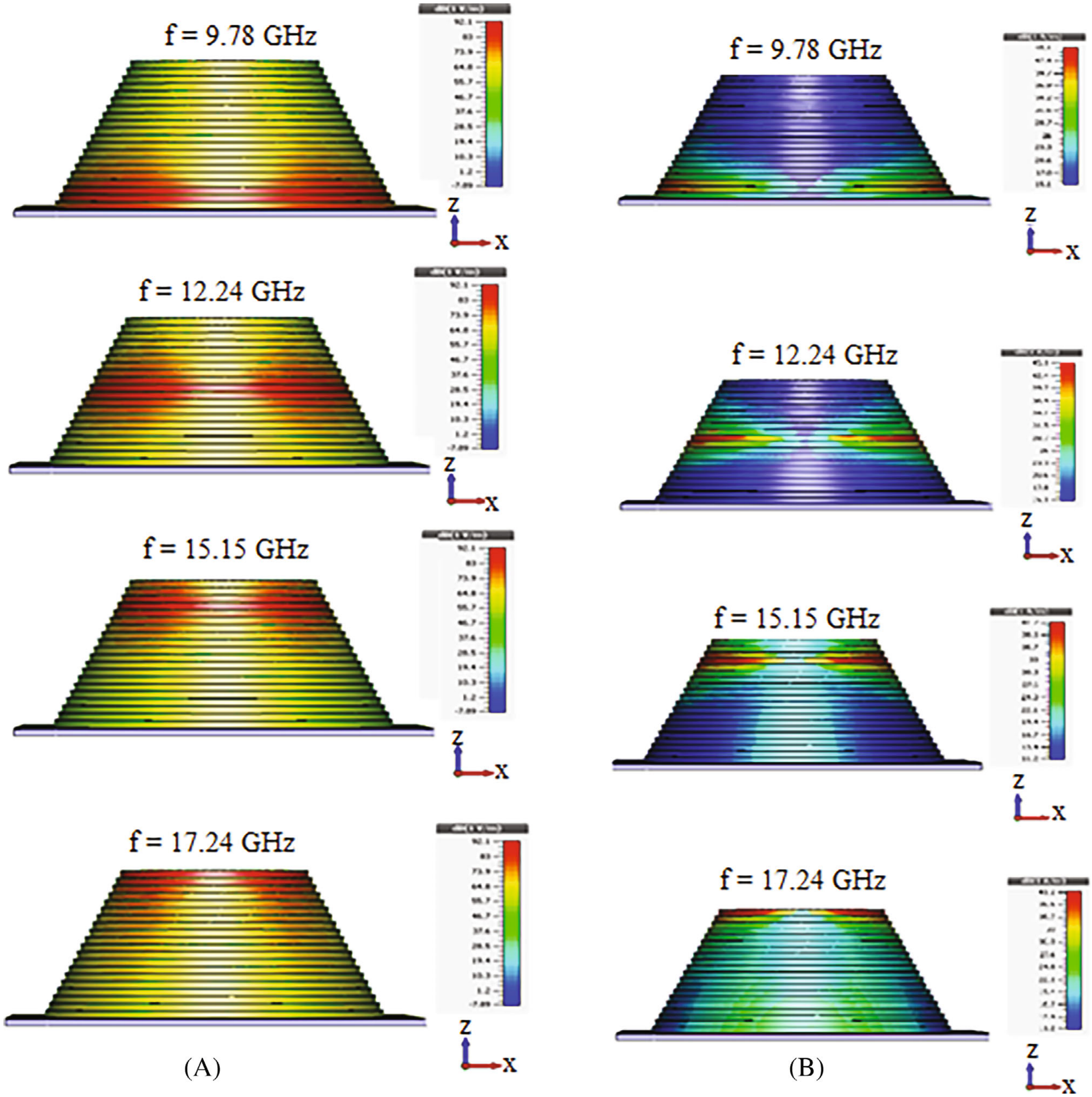

FIGURE 3 (A) Electric field distribution and (B) magnetic field distribution of proposed structure at 9.78, 12.24, 15.15, and 17.24 GHz, respectively.

simulation results of the electric and magnetic field amplitudes are obtained at 9.78, 12.24, 15.15, and 17.24 GHz. At a frequency of 9.78 GHz, the lowest frequency at which the structure resonates, the electric and magnetic fields are concentrated at the bottom side of the structure, which has the largest layer. As the resonant frequency increases, the electric and magnetic fields are concentrated in a layer having a smaller dimension. Since size and wavelength are correlated, long wavelengths (low frequencies) need larger sizes. The overall bandwidth of the structure is about 7.5 GHz, ranging from 10 to 17.5 GHz; that is, each layer extends the bandwidth by about 375 MHz.

The effects of the TE and TM polarized incident waves on the absorption performance of the structure are also analyzed and plotted in Figure 4. As depicted in Figure 4, the frequency response of the cone-based metamaterial absorber structure is almost insensitive to the polarization changes. On the other hand, the maximum absorption value corresponding to the TEM wave is also higher than 90% for the same frequency range. The suggested absorber's high

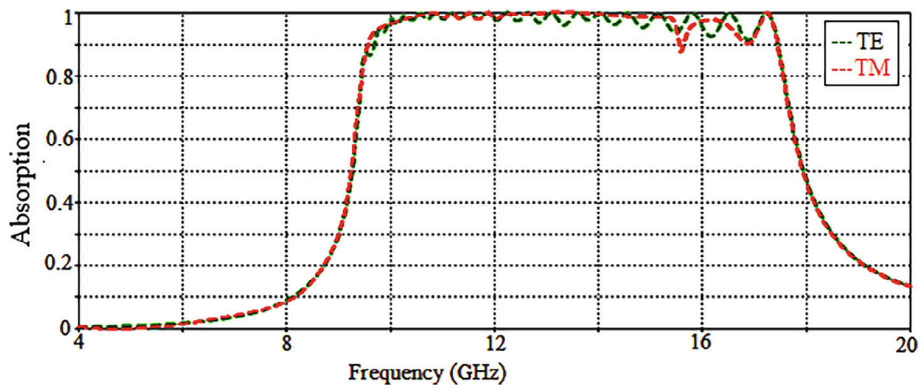

FIGURE 4 The absorption responses of the structure for TE and TM polarized waves.

absorption value distinguishes it from other structures in the literature due to its polarization-independent properties. The polarization-independent feature of the structure comes from the central symmetry of the structure for TE and TM incident cases. Due to its extremely wide absorption and reflection bandwidth and a high absorption value of over 90%, the proposed structure has great advantages, and therefore, for many applications, this structure could also find application areas such as stealth technology, energy harvesting, and solar energy. It can be noted that the performance of the resonator results from its novel structure.

The angular-dependent properties of a stepped cone-based metamaterial absorber structure in terms of azimuth (φ) and polar angle (θ) for TE and TM polarizations are also investigated. The azimuth angle dependency of the structure for TE and TM polarized waves is presented in Figure 5A,B, respectively. In Figure 5A, the absorption responses of the proposed structure for a TE polarized wave are demonstrated depending on the value of six different azimuth angles. A similar graph for the TM-polarized wave is shown in Figure 5B. The frequency responses of the structure are almost independent of the azimuth (φ) angle, ranging between 0° and 90° for both TE and TM polarized waves, as shown in Figure 5A,B. The independent properties of azimuth angle of the suggested absorber also distinguish this absorber from other broad-band absorbers in the literature. The azimuth angle independence characteristics for TE and TM polarized waves come from their symmetry with respect to the azimuth angle. The absorption value is almost over 90% in an extremely wide frequency band ranging from 10 to 17.5 GHz, as shown in Figure 5A,B.

The effects of polar angle on the frequency responses of the absorber for TE and TM polarized waves are also investigated and plotted, as shown in Figure 5C,D, respectively. The absorption values for the TE polarized wave are approximately acceptable, but for the TM polarized wave with a polar angle greater than 30°, large deviations were observed, as shown in Figure 5D, when compared with the results obtained for 0° of polar angle. Despite the reduced bandwidth, the 10–12 GHz band, which corresponds to half of the X band, is still covered. Hence, the proposed 3D stepped cone structure can be considered a novel metamaterial having not only polarization independent responses but also azimuth and polar angle independent characteristics within the frequency band covering the half of the X band in which stealth technology, cloaking, and energy harvesting applications are used.

Another alternative 3D multi-layer stepped structure is a pyramidal structure with a square cross section whose edge is equal to the radius of the corresponding circular layer forming the cone in the 3D structure. The pyramidal structure consists of 20 square layers of different sizes. Each layer is composed of a metal plate placed on a dielectric substrate. The bottom of the widest layer is also covered by a metal layer to block transmission, as in the case of a 3D stepped cone structure. Abroad band absorption response is also obtained for the 3D pyramidal structure. The polarization responses of both pyramidal and conical 3D structures are obtained for comparison purposes, and the results are shown in this simulation. In this case, the edge of the square forming the pyramid was taken to be equal to the radius of the circular layer forming the cone. The polarization responses of both 3D structures are shown in Figure 6A. As it is seen from Figure 6A–C, although the bandwidths corresponding to both structures are approximately equal, the absorption characteristics of the cone-type resonators are much better than those of the pyramid. The 2 GHz shift in resonance frequency is caused by the edges of the squares forming the pyramid. As seen in Figure 6B, the superior absorption properties of the 3D stepped cone over the 3D stepped pyramid come from the central symmetry of the cone. Hence, it can be concluded that although the pyramid type layered metamaterial absorber has a wide absorption band, as in the case of the cone type layered metamaterial absorber, the absorption level of the pyramid type layered metamaterial is not as good as that of the cone

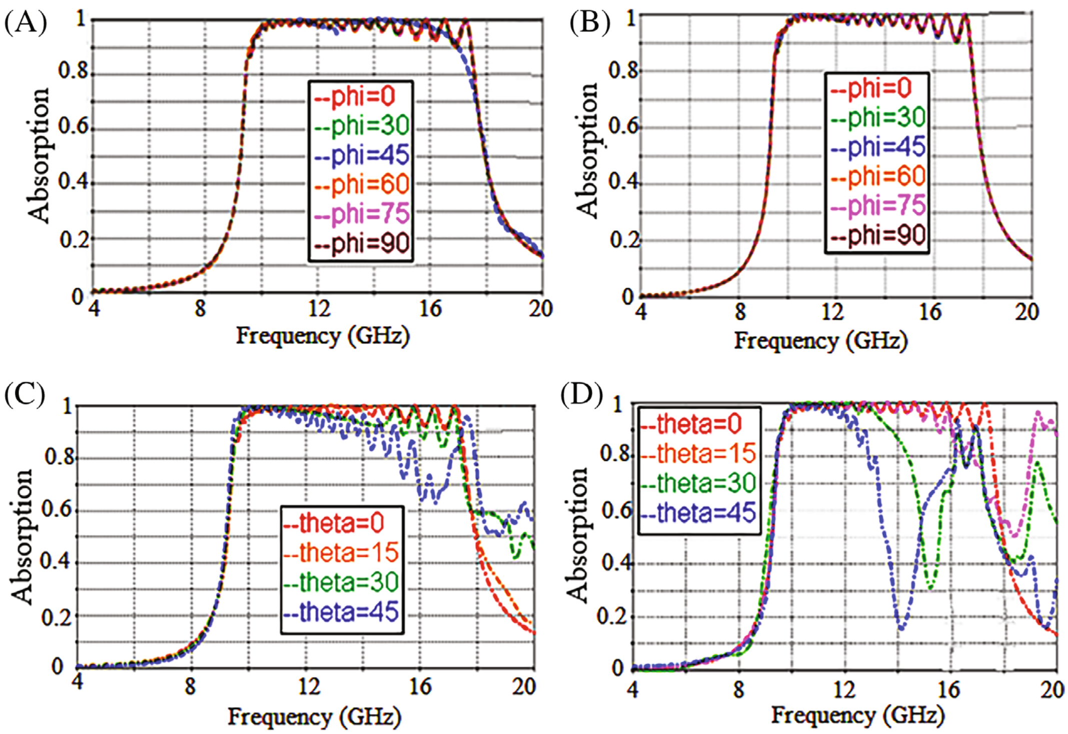

FIGURE 5 Angular dependency with respect to azimuth angle (A) TE polarized wave, (B) TM polarized wave. Angular dependency with respect to polar angle (C) TE polarized wave, (D) TM polarized wave.

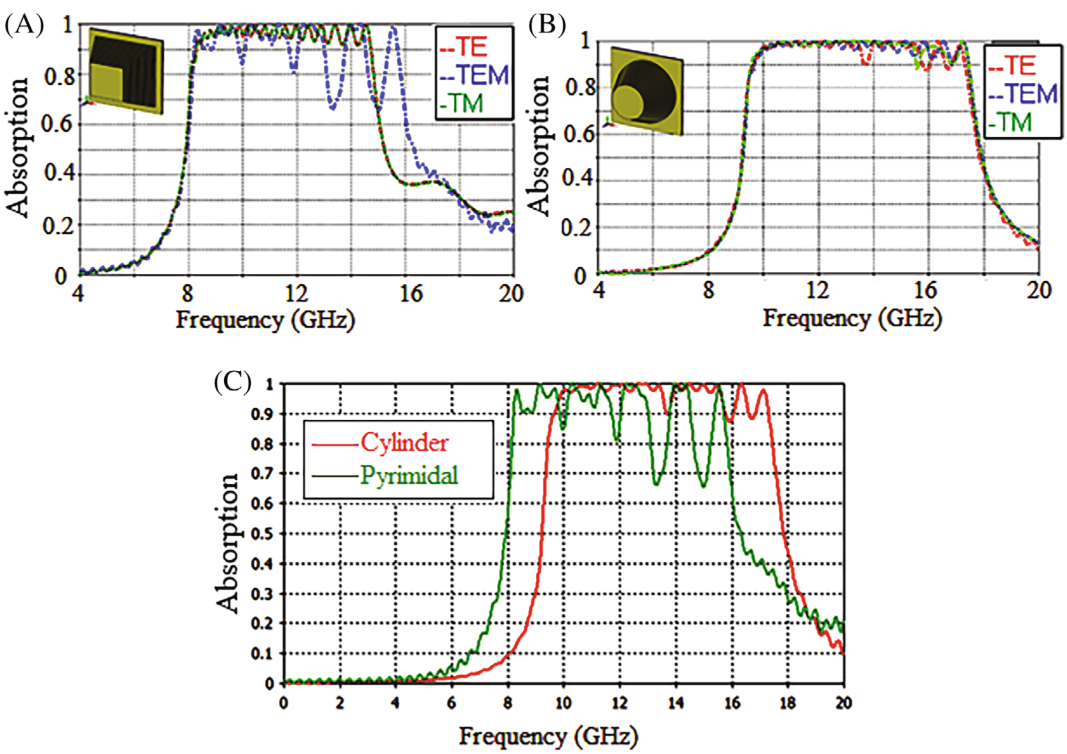

FIGURE 6 The absorption responses of (A) pyramid type layered structures, (B) cone type layered structures, and (C) both cone type and pyramid type layered structures.

type layered metamaterial within the entire bandwidth. Another important point to be noted is that the pyramid-type layered metamaterial is more sensitive to the polarization of the incident wave than the cone type layered metamaterial when Figure 6A is compared to the Figure 6B.

4 | ENERGY HARVESTING APPLICATION OF THE MULTI-LAYERED STEPPED CONE-STRUCTURED MA

To provide high-speed and broadband energy harvesting, it is required to obtain a structure that shows broadband absorption response. Hence, it is necessary to obtain metamaterials with high absorber characteristics. High absorption properties require some physical mechanisms. First, the good impedance matching between free space (377 Ω) and the intrinsic impedance of the proposed structure. The impedance matching provides exact penetration of the incident wave into the structure. The broadband absorption is only possible in cases of impedance matching throughout the overall frequency range. Second, when an EM wave is propagating along the structure, it must decay when traveling between front and back surfaces. Hence, the loss tangent of the structure must be sufficiently high. Lastly, the back surface of the structure must be exactly a conductor to prevent transmission and to provide travel for the EM wave between the front and back surfaces. In addition, these three conditions must be provided for the entire frequency range, that is, wavelength. The absorbed EM waves can be harvested using various mechanisms, such as AC-DC converters and rectifiers.

The proposed structure can be used in energy harvesting since it has the potential to absorb almost all incident energy within a wide frequency range. The electric and magnetic field vectors are oriented in the x and y directions, respectively, due to the symmetric nature of the absorber, to produce a TEM wave. The boundary conditions of metamaterial absorbers are crucial for optimizing their performance. Careful consideration of substrate properties, layer thickness, geometry, incident angle, polarization, and environmental conditions is essential in designing metamaterial absorbers for specific applications. The symmetry of the absorber structure and its angle- and polarization-independent nature provide an excellent harvesting application opportunity. For this reason, the boundary conditions are selected as perfectly electric conductor (PEC) in the x direction and perfectly magnetic conductor in the y direction. The modified version of the structure composed of four adjacent cones and boundary conditions are demonstrated in Figure 7A,B, respectively. This version includes four resonators to connect resistive loads between them. Resistive loads are considered lumped elements. To better realize the harvesting response of the structure, three resistive loads are placed between two adjacent cones: one of them is connected between the edges of the copper films on the bottom layers, the second one is connected between the copper films on the middle layers, and the last one is connected between the copper films on the top layer of the stepped cones. Hence, the absorbed EM energy in the structure will be converted into usable electric energy.

To explain the physical mechanism of the absorber, the conversion (CE), absorption (AE), and harvesting efficiencies (HE) are extracted by using the Equations (3)–(5) given below.

Conversion efficiency defines part of the penetrated power (PA) that can be turned into electric power by using lumped resistor (PR).

$$CE = (PR/PA) \times 100. \tag{3}$$

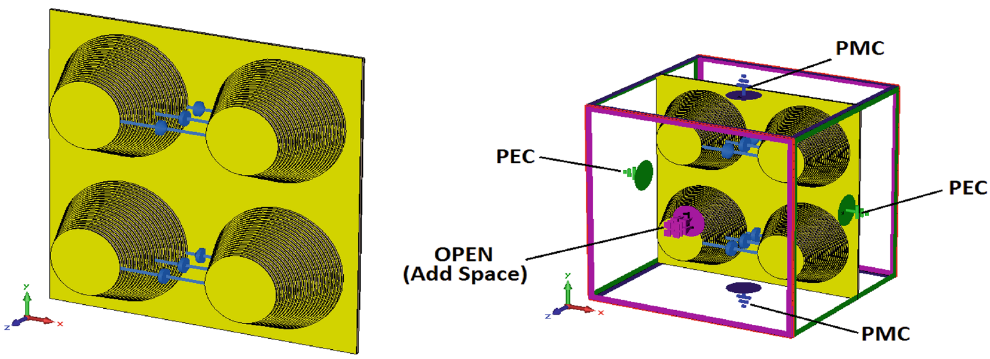

(A) (B)

FIGURE 7 Modified version of proposed structure with resistive loads (A) unit cell and (B) boundary conditions.

Harvesting efficiency denotes to the simulated power (PS) which can be transformed into electric power (PR) by using lumped resistors.

$$HE = (PR/PS) \times 100. \tag{4}$$

Absorption efficiency is the power percentage of the incident wave successfully absorbed by the material. Therefore, it is the ratio of accepted power (PR) and the simulated power (PA).

$$AE = (PA/PS) \times 100. \tag{5}$$

The value of each resistor is determined by parametric study in simulations and selected as 250 Ω to satisfy the impedance matching condition. To better analyze the potential use of the structure, the frequency response of the resistors, including the accepted power through resonators and stimulated power to the structure, is calculated for the frequency band ranging from 4 to 20 GHz, and the results are shown in Figure 8. It can be seen that the accepted power and consumption power have equal amplitude, with a range of 50%–83% efficiency within 4 and 8.5 GHz. Figure 8 shows that the structure transfers accepted power to resistive loads with very little loss. Hence, the structure can be used as a harvester even in this lower frequency range, although this frequency band is not covered within the bandwidth of the absorber structure. It means that conversion efficiency (CE) is very high in this frequency interval (CE > 90%). But the same argument is not valid in the 8.50–11.50 GHz range. Although the frequency response of accepted power is around 90%, the consumed power is not so much. In Figure 8, the absorption characteristics of structure and accepted power are also demonstrated in the same frequency interval (4–20 GHz). As it is shown in Figure 8, the absorption and the accepted power through all resonators are equal in magnitude for all frequencies within the operation ranges of the structure. This means that the proposed structure has perfect absorber characteristics. In addition, an increase in the number of resistors can enhance the total power loss in the structure. Hence, it can be concluded that the harvesting efficiency of the structure can be enhanced by increasing the number of lumped elements.

By using the equations given above, important marker values such as CE, HE, and AE of the harvesting potential of the structure are evaluated, as shown in Figure 9. The CE is almost over 90% up to 8.5 GHz, as discussed above. Although the absorption efficiency of the proposed structure gradually increases, the harvesting efficiency of the proposed structure tends to decrease between 8.5 and 10.74 GHz. So the conversion efficiency decreases in these frequency ranges and reaches its minimum value of 20.85% at 10.74 GHz. Although the absorption efficiency of the proposed structure remains approximately constant over a frequency range of 10.74–11.62 GHz, the harvesting efficiency of the structure increases. Therefore, the conversion efficiency increases in these frequency ranges. The conversion efficiency reaches its maximum value (79.74%) at 11.98 GHz because the absorption and harvesting efficiencies have the same responses in this interval ranging from 11.62 to 11.98 GHz. Although there may be some small fluctuations in absorption efficiency, harvesting and conversion efficiencies are both decreasing within the range of 11.98–16.2 GHz and then increasing within the range of 16.2–20 GHz. Conversion efficiency reaches its maximum value of 81.27% at 18.62 GHz. It should be noted that the proposed structure can be used as a harvester with very high absorption efficiency (over 80%) within the 8–20 GHz frequency band.

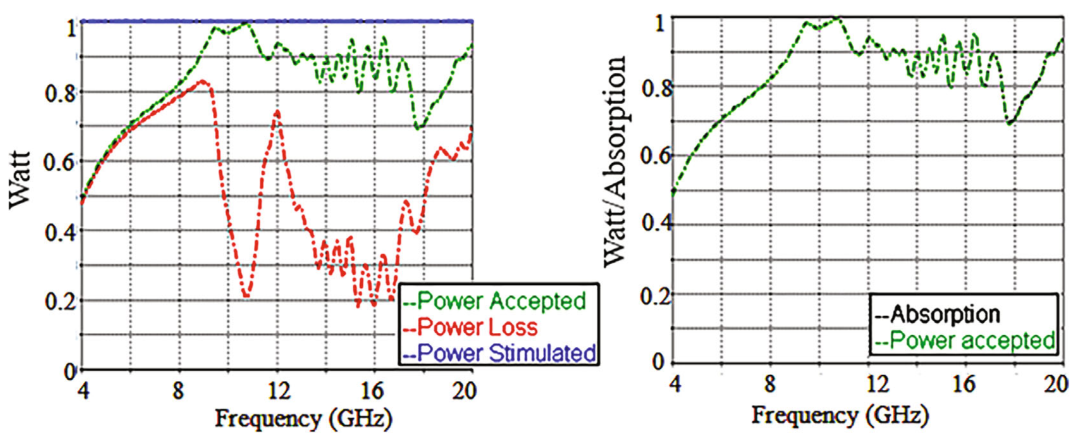

FIGURE 8 Loss power, accepted power, stimulated power, and absorption.

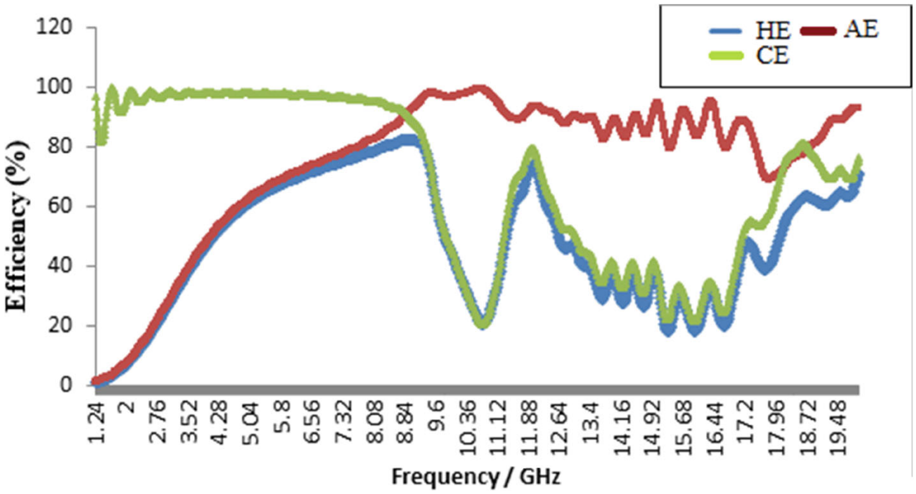

FIGURE 9 Harvesting, absorption, and conversion efficiency of the structure.

TABLE 1 Efficiency level of structure.

Sample	Frequency (GHz)	Absorption efficiency (%)	Harvesting efficiency (%)	Conversion efficiency (%)	Absorption level	Harvesting level	Conversion level
1	8.86	90.51	82.74	91.41	High	High	High
2	10.74	99.52	20.75	20.85	High	Low	Low
3	11.62	89.24	62.94	70.54	High	Medium	Medium
4	11.98	93.36	74.44	79.74	High	Medium	Medium
5	18.62	77.61	63.08	81.28	Medium	Medium	High
6	20	93.04	71.16	76.49	High	Medium	Medium
	80–100: High		60–80: Medium		0–60: Low		

To better understand the absorption, harvesting, and conversion levels of the proposed structure, some absorption, harvesting, and conversion efficiency magnitudes of the proposed structure are selected and listed in Table 1. If the absorption and harvesting efficiencies are sufficiently high, the conversion efficiency will also be high, corresponding to sample 1. For sample 2, when the absorption efficiency is high and the harvesting efficiency is low, the conversion efficiency is also low. As shown in the third row of Table 1, from the data corresponding to Sample 3, the harvesting efficiency determines the level of the conversion efficiency. Other possibilities can be found using the following formula and descriptions.

$$\mathrm{CE} = (\mathrm{HE}/\mathrm{AE}) * 100. \tag{6}$$

For example, AE = High, HE = Medium → CE = Medium/High = Medium (sample 4) and AE = Medium, HE = Medium → CE = Medium/Medium = High (sample 5).

According to the mentioned samples, the suggested absorber is more appropriate with respect to the others in the literature for absorber applications due to its high absorption, harvesting, and conversion efficiency characteristics.

5 | STEALTH APPLICATION OF THE MULTI-LAYERED STEPPED CONE-STRUCTURED MA

The proposed structure can be used in many areas, like medical imaging, satellite communication, sensor application, and so on. Additionally, the proposed structure can be configured by using terahertz, optical frequencies, and infrared. In this

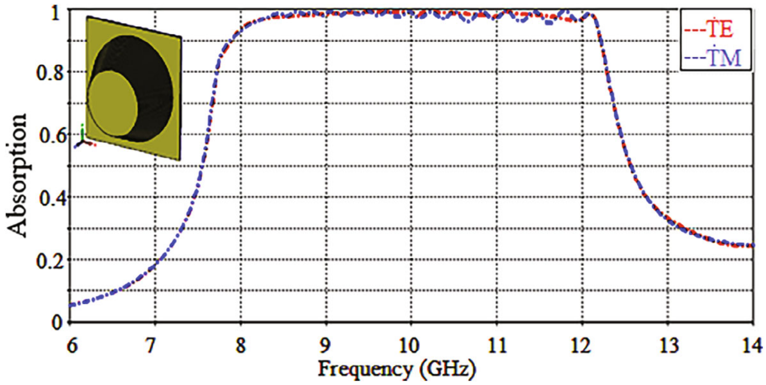

FIGURE 10 Absorption graph of modified structure for TE and TM incident cases.

part, the stealth technology application of the proposed structure for military radars in the X band (short-range tracking, missile guidance, mapping, marine radar, and airborne intercept) is investigated. Since the proposed structure has high absorption with polarization and angular independence characteristics, it can be useful for stealth applications in the X-band with operation frequencies ranging from 8 to 12 GHz. In order to operate in the X band, the proposed structure shown in Figure 1B should be resized. The modified dimensions $a = 7$ mm, $b = 10.99$ mm, and $c = 13$ mm will ensure that the proposed structure operates in the X band, and there is no need to change the other dimensions. The changed dimensions of the absorber are evaluated using a genetic algorithm and a parametric study. The absorption graph of the modified structure for X-band radars is demonstrated in Figure 10. The modified structure has high absorptivity between 8 and 12 GHz for both TE and TM incident cases. Although the absorption level is about 93% at some frequencies, the absorption level at normal incidence is generally above 95% in the frequency range of 8–12 GHz. The stealth application is also polarization independent in the X band for TE and TM incident cases. Hence, the structure is an ideal novel candidate for future stealth and cloaking technologies with high performance and polarization independence.

6 | FABRICATION AND MEASUREMENT

The proposed structure is fabricated to verify the absorption efficiency and to demonstrate the convenience between measurement and simulation. For fabrication, we use dielectric and metal, which have the same properties with numerically designed structures. Besides, the thicknesses of FR-4 and copper are 1.6 and 0.035, respectively. All dimensions of a structure are the same in simulations. Due to the limitations in facilities, the fabrication is carried out for one layer of structure, and the numerical analysis is also designed to be convenient with a fabricated sample. We only fabricate the ground layer and the first circle layer due to the difficulty of bonding and cutting 20 dielectric and metal layers with varying dimensions (from 5 to 8 mm). The fabricated structure consists of a ground plane and 10×10 circle dielectric and metal layers, which are demonstrated in Figure 11A. In order to show that the simulation result matches up with the experimental result, we have compared the experimental and simulation results of the structure, which consists of the first circle layer. As previously stated, the diameter of the first circle layer is 8.99 mm. The measurement has been realized by using a vector network analyzer (VNA) and two horn antennas with broadband and high gain characteristics (Figure 11B). Agilent's 2-Port PNA-L network analyzer is used with a frequency range of 10 MHz to 43.5 GHz. Measurements are conducted by using two horn antennas working from 4 to 20 GHz in our microwave laboratory. The measured maximum absorption rate is around 0.35 at 9.5 GHz for a one-layer structure. The measurement results are in good agreement with the numerical analysis in the one-layer case. Due to calibration errors, there is an inequality between simulation and experimental results. The difference between the experimental results and the theoretical ones stems from the measurement medium. Although the free space measurements can be carried out in an anechoic chamber to provide a good match, the measurements are realized in free space. The scattering from the measurement environment and losses due to unavoidable structures in the laboratory medium result in a difference between measurement and simulation. Experimental results are compatible with simulation results. Hence, it can be concluded that the fabrication of an exact cone also provides nearly the same broad band absorption with high efficiency in line with numerical analysis.

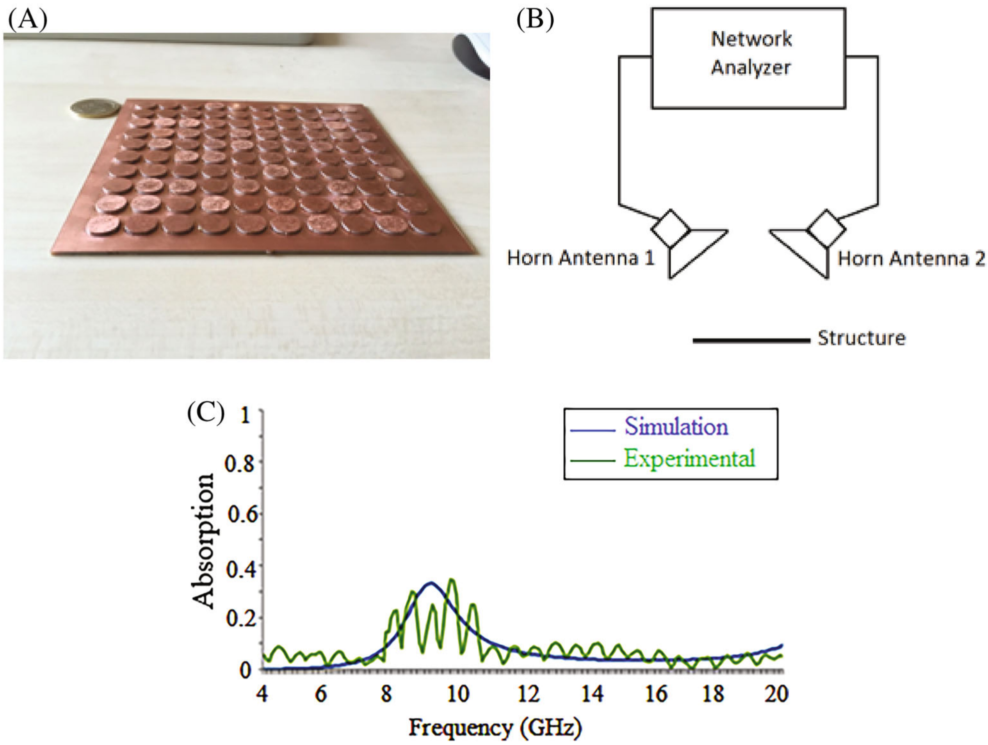

FIGURE 11 (A) Fabricated sample, (B) measurement setup, and (C) absorption comparison with fabricated structure.

7 | CONCLUSION

In conclusion, a wide band absorber is investigated in the case of electromagnetic wave absorption and harvesting in the microwave range. This structure presents areas of application for stealth technology. The simulation results demonstrate that the designed absorber has nearly perfect absorption over 90% between the 9.68 and 17.45 GHz frequency regions. Furthermore, the absorption level is greater than 95% in the frequency range of 9.91–14.86 GHz, indicating the potential for harvesting applications. The simulation results show that the proposed structure also has polarization and angular independence for both TE and TM incident waves. The high level of absorption, wide bandwidth characteristic, incident angle, and polarization independence of the structure distinguish it from other studies in the literature. When the unique features of this structure are taken into account, the proposed cone metamaterial absorber is a novel candidate for cloaking and stealth technologies in the X band. In addition, the cone based harvester has a potential for energy conversion in the frequency band of satellite communication. As a result, the 3D stepped cone metamaterial absorber can be a good candidate for future energy harvesting, stealth technology, and cloaking systems.

AUTHOR CONTRIBUTIONS

Mehmet Bağmancı: Conceptualization; investigation; writing – original draft; methodology; software; data curation; visualization. **Lulu Wang:** Methodology; validation; visualization; formal analysis; project administration; writing – review and editing; data curation; supervision. **Cumali Sabah:** Conceptualization; data curation; supervision; resources; writing – review and editing; funding acquisition; writing – original draft; investigation. **Muharrem Karaaslan:** Conceptualization; investigation; funding acquisition; writing – original draft; writing – review and editing; software; formal analysis; project administration; supervision; data curation; resources. **Liton Chandra Paul:** Conceptualization; investigation; funding acquisition; writing – review and editing; visualization; supervision; data curation; resources; formal analysis; project administration; software; validation. **Tithi Rani:** Funding acquisition; writing – original draft; writing – review and editing; visualization; validation; formal analysis; data curation; software; resources. **Emin Unal:** Conceptualization; methodology; software; data curation; supervision; resources; project administration; visualization; investigation; writing – original draft.

CONFLICT OF INTEREST STATEMENT

The authors declare no conflict of interest.

PEER REVIEW

The peer review history for this article is available at https://www.webofscience.com/api/gateway/wos/peer-review/10.1002/eng2.12903.

DATA AVAILABILITY STATEMENT

The data that support the findings of this study are available from the corresponding author upon reasonable request.

ORCID

Mehmet Bağmancı https://orcid.org/0000-0001-6996-958X
Lulu Wang https://orcid.org/0000-0001-7466-9522
Cumali Sabah https://orcid.org/0000-0002-4346-3537
Muharrem Karaaslan https://orcid.org/0000-0003-0923-1959
Liton Chandra Paul https://orcid.org/0000-0001-6184-7350
Tithi Rani https://orcid.org/0000-0002-0897-1579
Emin Unal https://orcid.org/0000-0002-4088-8353

REFERENCES

1. Cao Y, Ruan C, Chen K, Zhang X. Research on a high-sensitivity asymmetric metamaterial structure and its application as microwave sensor. *Sci Rep*. 2022;12(1):1-20.
2. Paul LC, Haque MA, Sarker S, Rashid MMU, Haque MA, Roy TK. Design and performance exploration of a DGS metamaterial MPA by etching four dual isosceles triangular defects on the ground plane. *2018 International Conference on Computer, Communication, Chemical, Material and Electronic Engineering (IC4ME2)*. IEEE; 2018:1-4.
3. Bakir M, Karaaslan M, Dincer F, Akgol O, Sabah C. Electromagnetic energy harvesting and density sensor application based on perfect metamaterial absorber. *Int J Mod Phys B*. 2016;30(20):1650133.
4. Feng Q, Zheng D, Liu Y, Lin YS. Tunable terahertz spiral-shaped metamaterial with single-to triple-resonance and polarization-dependence characteristics. *Appl Phys A*. 2022;128(6):1-8.
5. Zhang T, Duan Y, Liu J, et al. Asymmetric electric field distribution enhanced hierarchical metamaterials for radar-infrared compatible camouflage. *J Mater Sci Technol*. 2022;146:10-18.
6. Quan C, Zou J, Guo C, Xu W, Zhu Z, Zhang J. High-temperature resistant broadband infrared stealth metamaterial absorber. *Opt Laser Technol*. 2022;156:108579.
7. Lee N, Lim JS, Chang I, Bae HM, Nam J, Cho HH. Flexible assembled metamaterials for infrared and microwave camouflage. *Adv Opt Mater*. 2022;10:2200448.
8. Hossain MB, Faruque MRI, Islam MT, Singh M, Jusoh M. Triple band microwave metamaterial absorber based on double E-shaped symmetric split ring resonators for EMI shielding and stealth applications. *J Mater Res Technol*. 2022;18:1653-1668.
9. Liu Y, Sun F, Yang Y, Hao Y, Liang S, Wang Z. A metamaterial-free omnidirectional invisibility cloak based on thrice transformations inside optic-null medium. *Opt Laser Technol*. 2023;157:108779.
10. Xu RJ, Lin YS. Actively MEMS-based tunable metamaterials for advanced and emerging applications. *Electronics*. 2022;11(2):243.
11. Luo X, Xiang P, Yu H, Huang S, Yu T, Zhu YF. Terahertz metamaterials broadband perfect absorber based on molybdenum disulfide. *IEEE Photon Technol Lett*. 2022;34(20):1100-1103.
12. Li Z, Cheng Y, Luo H, Chen F, Li X. Dual-band tunable terahertz perfect absorber based on all-dielectric InSb resonator structure for sensing application. *J Alloys Compd*. 2022;925:166617.
13. Jiang L, Yi Y, Tang Y, et al. A high-quality-factor ultra-narrowband perfect metamaterial absorber based on monolayer molybdenum disulfide. *Chin Phys B*. 2022;31(3):038101.
14. Li Y, Lin C, Li K, Chi C, Huang B. Nanoparticle-on-mirror metamaterials for full-spectrum selective solar energy harvesting. *Nano Lett*. 2022;22(14):5659-5666.
15. Persis GE, Paul JJ, Mary TB, Joy RC. A compact tilted split ring multiband metamaterial absorber for energy harvesting applications. *Mater Today Proc*. 2022;56:368-372.
16. Shuvo MMK, Hossain MI, Mahmud S, et al. Polarization and angular insensitive bendable metamaterial absorber for UV to NIR range. *Sci Rep*. 2022;12(1):1-15.
17. Shen S, Liu X, Shen Y, et al. Recent advances in the development of materials for terahertz metamaterial sensing. *Adv Opt Mater*. 2022;10(1):2101008.
18. Elmahaishi MF, Ismail I, Muhammad FD. A review on electromagnetic microwave absorption properties: their materials and performance. *J Mater Res Technol*. 2022;20:2188-2220.
19. Qu S, Sheng P. Microwave and acoustic absorption metamaterials. *Phys Rev Appl*. 2022;17(4):047001.

20. Mei H, Yang W, Yang D, et al. Metamaterial absorbers towards broadband, polarization insensitivity and tunability. *Opt Laser Technol*. 2022;147:107627.
21. Zhao Y, Hao L, Zhang X, et al. A novel strategy in electromagnetic wave absorbing and shielding materials design: multi-responsive field effect. *Small Sci*. 2022;2(2):2100077.
22. Al-badri KSL. Electromagnetic broad band absorber based on metamaterial and lumped resistance. *J King Saud Univ Sci*. 2020;32(1):501-506.
23. Ullah N, Islam MS, Hoque A, et al. A compact complementary split ring resonator (CSRR) based perfect metamaterial absorber for energy harvesting applications. *Eng Sci Technol Int J*. 2023;45:101473.
24. Lee G, Lee SJ, Rho J, Kim M. Acoustic and mechanical metamaterials for energy harvesting and self-powered sensing applications. *Mater Today Energy*. 2023;37:101387.
25. Xiao H, Li T, Zhang L, Liao WH, Tan T, Yan Z. Metamaterial based piezoelectric acoustic energy harvesting: electromechanical coupled modeling and experimental validation. *Mech Syst Sign Process*. 2023;185:109808.
26. Ju Z, Wen J, Shi L, et al. Ultra-broadband high-efficiency airy optical beams generated with all-silicon metasurfaces. *Adv Opt Mater*. 2021;9(1):2001284.
27. Cai B, Wu L, Zhu X, Cheng Z, Cheng Y. Ultra-broadband and wide-angle plasmonic light absorber based on all-dielectric gallium arsenide (GaAs) metasurface in visible and near-infrared region. *Results Phys*. 2024;58:107509.
28. Rong C, Cai B, Cheng Y, Chen F, Luo H, Li X. Dual-band terahertz chiral metasurface absorber with enhanced circular dichroism based on temperature-tunable InSb for sensing applications. *Phys Chem Chem Phys*. 2024;26:5579-5588.
29. Lv Z, Li Z, Han Y, Cao Y, Yang L. A wideband and ultra-thin metamaterial absorber based on resistive FSS. *Symmetry*. 2022;14(6):1148.
30. Guo L, Wang Z, Zeng W, Hou S, Yang Z, Liu Y. A compact and high gain metalens antenna based on impedance matching mechanism. *AEU Int J Electron Commun*. 2022;146:154113.

How to cite this article: Bağmancı M, Wang L, Sabah C, et al. Broadband multi-layered stepped cone shaped metamaterial absorber for energy harvesting and stealth applications. *Engineering Reports*. 2024;6(11):e12903. doi: 10.1002/eng2.12903